

## Supporting Information

# Rhenium(I) Tricarbonyl Complexes with Peripheral *N*-Coordination Sites: a Foundation for Heterotrimetallic Nonlinear Optical Chromophores

Benjamin J. Coe,<sup>†</sup> Simon P. Foxon,<sup>†</sup> Rachel A. Pilkington,<sup>†</sup> Sergio Sánchez,<sup>†</sup> Daniel Whittaker,<sup>†,‡</sup> Koen Clays,<sup>‡</sup> Nick Van Steerteghem,<sup>‡</sup> and Bruce S. Brunshaw<sup>§</sup>

<sup>†</sup> *School of Chemistry, The University of Manchester, Oxford Road, Manchester M13 9PL, U.K.*

<sup>‡</sup> *Department of Chemistry, University of Leuven, Celestijnenlaan 200D, B-3001 Leuven, Belgium*

<sup>§</sup> *Molecular Materials Research Center, Beckman Institute, MC 139-74, California Institute of Technology, 1200 East California Boulevard, Pasadena, California 91125*

<sup>‡</sup> *Present address: National Nuclear Laboratory, Sellafield, Seascale, Cumbria CA20 1PG, U.K.*

1. Additional Crystallographic Data .....	S2
2. Additional <sup>1</sup> H NMR Spectroscopic Data .....	S3
3. Additional Electrochemical and Spectroelectrochemical Data .....	S4
4. Additional Electronic Absorption and Emission Spectroscopic Data .....	S7

## 1. Additional Crystallographic Data

**Table S1. Crystallographic Data and Refinement Details for Solvates of 1–6**

	1·Me <sub>2</sub> CO	2·PhMe	3·0.5PhMe	4·0.5Me <sub>2</sub> CO	5·0.5PhMe	6·MeCN
empirical formula	C <sub>18</sub> H <sub>12</sub> ClN <sub>4</sub> O <sub>4</sub> Re	C <sub>25</sub> H <sub>17</sub> F <sub>3</sub> N <sub>5</sub> O <sub>6</sub> ReS	C <sub>24.5</sub> H <sub>15</sub> F <sub>3</sub> N <sub>5</sub> O <sub>6</sub> ReS	C <sub>23.5</sub> H <sub>13</sub> F <sub>3</sub> N <sub>6</sub> O <sub>6.5</sub> ReS	C <sub>31</sub> H <sub>18</sub> ClN <sub>4</sub> O <sub>3</sub> Re	C <sub>32</sub> H <sub>20</sub> F <sub>3</sub> N <sub>6</sub> O <sub>6</sub> ReS
fw	569.97	758.70	750.67	758.66	716.14	859.80
cryst system	monoclinic	triclinic	orthorhombic	triclinic	monoclinic	monoclinic
space group	<i>P</i> 2 <sub>1</sub> / <i>c</i>	<i>P</i> $\bar{1}$	<i>Pb</i> <i>cn</i>	<i>P</i> $\bar{1}$	<i>P</i> 2 <sub>1</sub> / <i>c</i>	<i>P</i> 2 <sub>1</sub> / <i>n</i>
<i>a</i> /Å	6.7065(4)	9.8664(5)	20.920(1)	10.602(1)	7.0510(8)	14.9062(5)
<i>b</i> /Å	24.786(1)	10.8251(6)	14.1928(6)	12.0951(9)	23.671(3)	15.4034(4)
<i>c</i> /Å	12.0178(6)	13.6341(7)	18.5858(8)	12.4270(8)	15.021(2)	16.6113(5)
<i>a</i> /deg	90.00	70.788(5)	90	89.784(6)	90	90
<i>β</i> /deg	100.237(5)	80.269(4)	90	66.738(8)	92.193(9)	102.651(3)
<i>γ</i> /deg	90.00	76.658(4)	90	67.606(8)	90	90
<i>U</i> /Å <sup>3</sup>	1965.8(2)	1331.1(1)	5518.3(4)	1333.2(2)	2505.2(5)	3721.5(2)
<i>Z</i>	4	2	8	2	4	4
<i>T</i> /K	101(2)	100(2)	150(2)	150(2)	150(2)	150(2)
<i>μ</i> /mm <sup>−1</sup>	6.349	4.715	4.548	4.709	5.001	3.383
cryst size/mm	0.1 × 0.1 × 0.05	0.4 × 0.2 × 0.05	0.1 × 0.02 × 0.02	0.25 × 0.1 × 0.1	0.1 × 0.1 × 0.1	0.35 × 0.08 × 0.08
cryst description	red rhombohedron	yellow plate	orange needle	light red needle	light yellow block	yellow needle
reflns collected	6760	9086	15277	8303	14375	13112
independent reflns	3596 (0.0494)	5640 (0.0389)	5876 (0.0567)	4838 (0.0445)	5108 (0.1352)	7541 (0.0412)
( <i>R</i> <sub>int</sub> )						
<i>θ</i> <sub>max</sub> /deg	25.35 (99.9)	26.73 (99.7)	28.64 (99.3)	25.35 (99.1)	26.37 (99.8)	26.38 (99.4)
(completeness)						
reflns with <i>I</i> > 2σ( <i>I</i> )	2824	5103	3534	4013	2889	5604
GOF on <i>F</i> <sup>2</sup>	1.099	1.080	1.104	1.047	0.948	1.070
final <i>R</i> 1, <i>wR</i> 2 [ <i>I</i> > 2σ( <i>I</i> )]	0.0544, 0.1145	0.0381, 0.0808	0.0527, 0.0749	0.0472, 0.0762	0.0751, 0.0975	0.0586, 0.1494
(all data)	0.0753, 0.1249	0.0441, 0.0865	0.1122, 0.1013	0.0639, 0.0853	0.1554, 0.1240	0.0844, 0.1679
peak and hole/eÅ <sup>−3</sup>	2.82, −1.39	2.12, −2.20	2.27, −1.25	1.11, −0.86	1.26, −0.88	4.68, −1.62

## 2. Additional $^1\text{H}$ NMR Spectroscopic Data

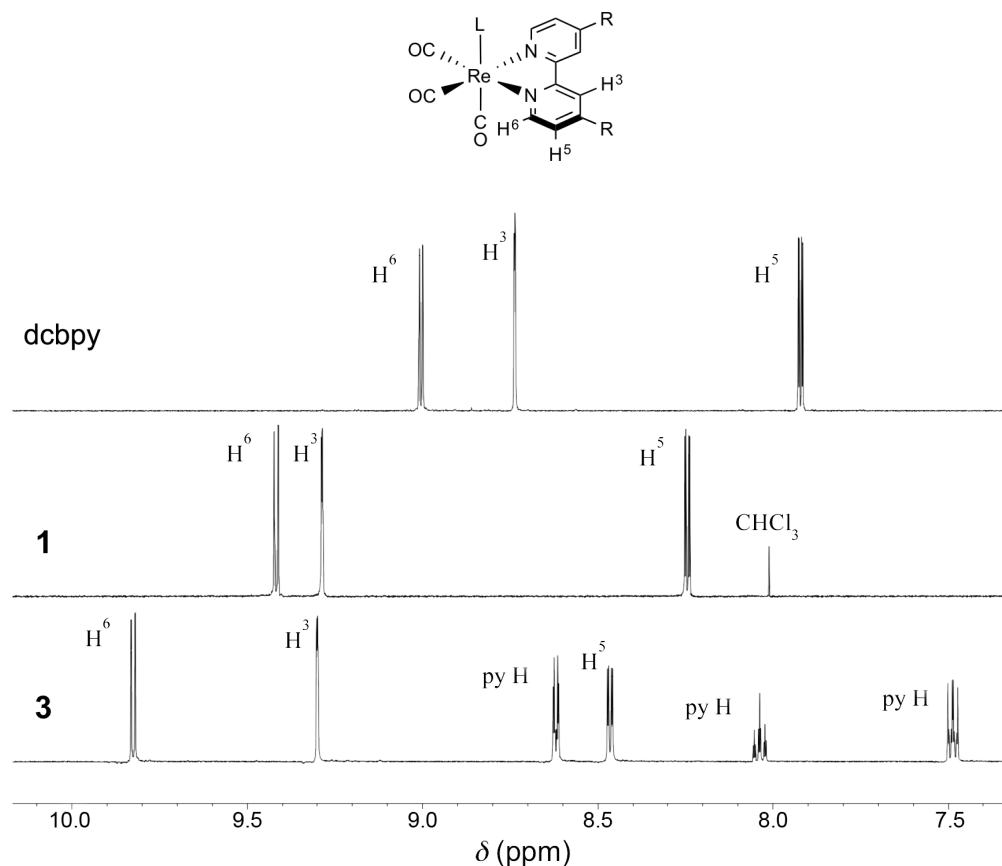


**Figure S1.**  $^1\text{H}$  NMR spectra of dcbpy, **1** and **3** (500 MHz in  $(\text{CD}_3)_2\text{CO}$  at 293 K). Complexing to a  $\text{fac-Re}^{\text{I}}\text{Cl}(\text{CO})_3$  center induces large downfield shifts of all signals, while substituting the  $\text{Cl}^-$  ligand with py causes further such shifts, although that for the  $\text{H}^3$  signal is only slight.

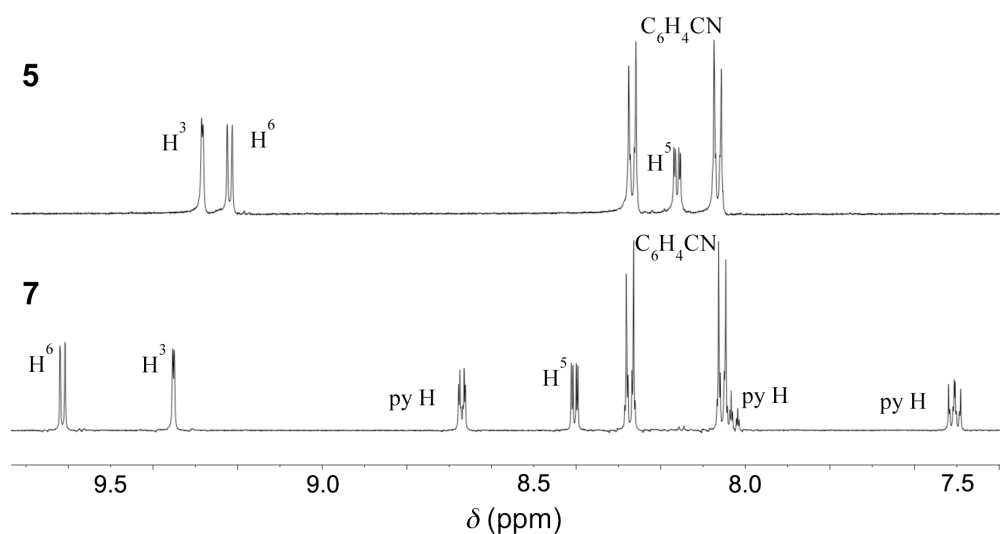


**Figure S2.**  $^1\text{H}$  NMR spectra of **5** and **7** (500 MHz in  $(\text{CD}_3)_2\text{CO}$  at 293 K). Replacing the  $\text{Cl}^-$  ligand with py shifts the signals for the bpy unit downfield (especially the  $\text{H}^5$  and  $\text{H}^6$  signals), while those for the benzonitrile fragments are essentially invariant.

### 3. Additional Electrochemical and Spectroelectrochemical Data

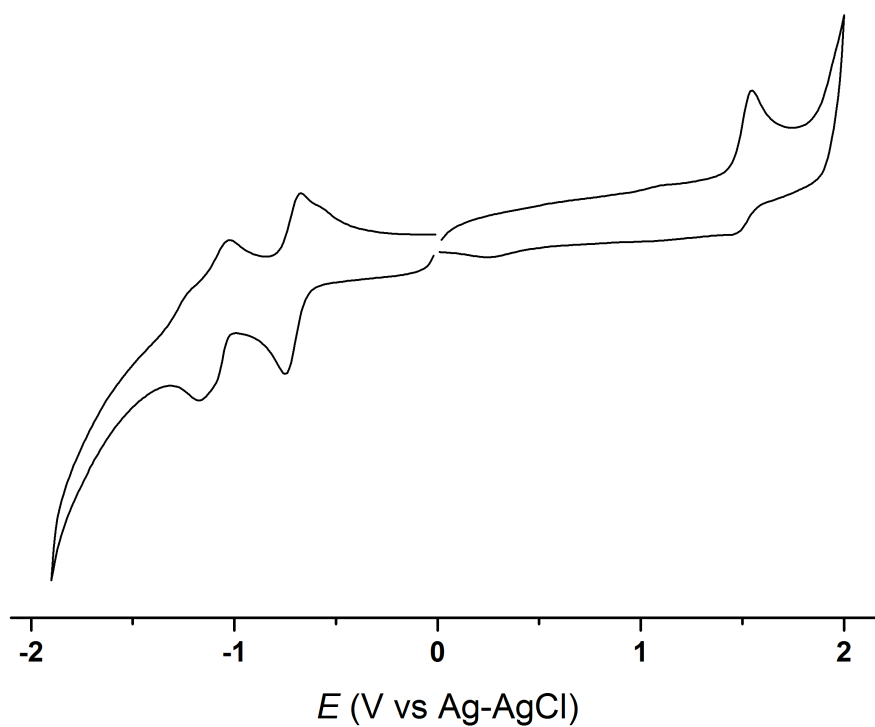


**Figure S3.** Cyclic voltammogram of complex **1** recorded at  $100 \text{ mV s}^{-1}$  in MeCN 0.1 M in  $[\text{N}(\text{C}_4\text{H}_9-n)_4]\text{PF}_6$  at 293 K.

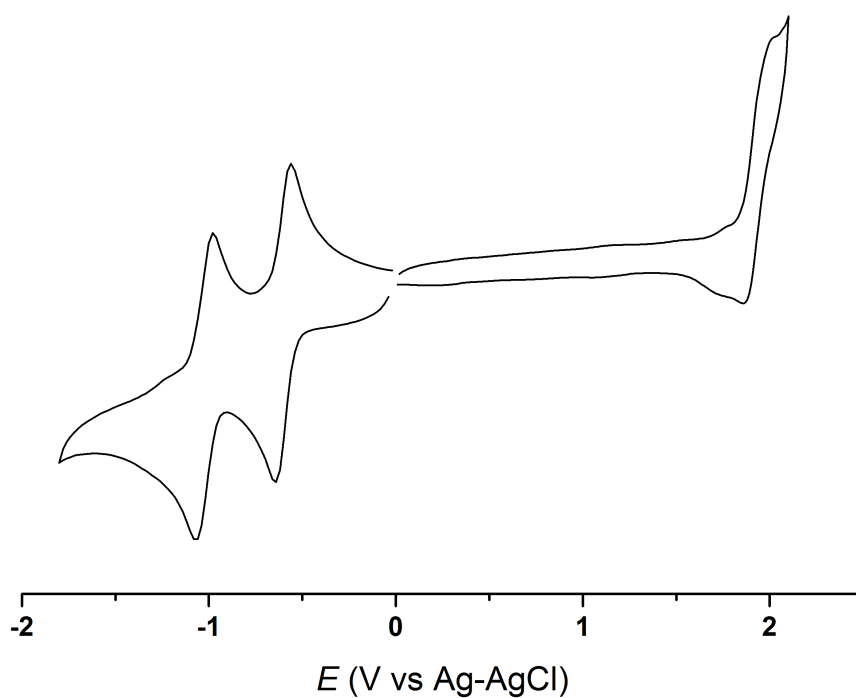


**Figure S4.** Cyclic voltammograms of complex salt **2** recorded at  $100 \text{ mV s}^{-1}$  in MeCN 0.1 M in  $[\text{N}(\text{C}_4\text{H}_9-n)_4]\text{PF}_6$  at 293 K.

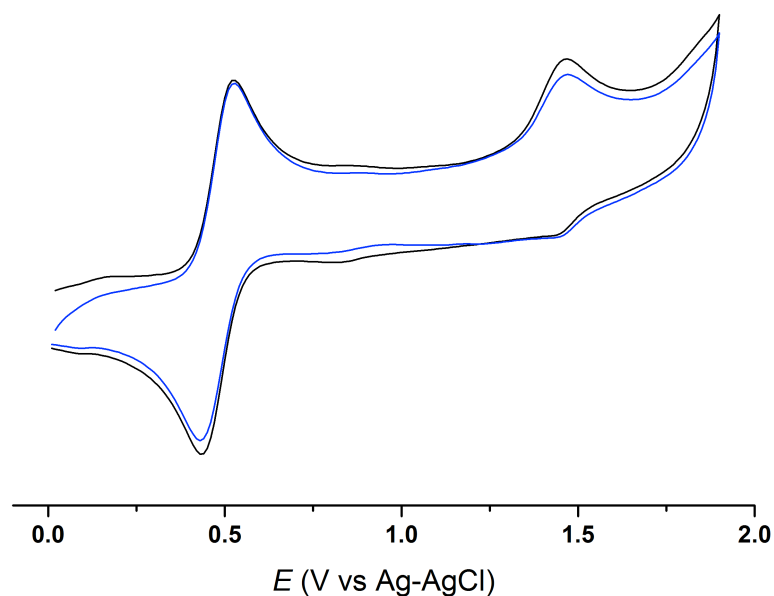


**Figure S5.** Cyclic voltammograms depicting the 1<sup>st</sup> (black) and 2<sup>nd</sup> (blue) scan for the oxidation processes of complex salt **11** recorded at 100 mV s<sup>-1</sup> in MeCN 0.1 M in [N(C<sub>4</sub>H<sub>9</sub>-*n*)<sub>4</sub>]PF<sub>6</sub> at 293 K.

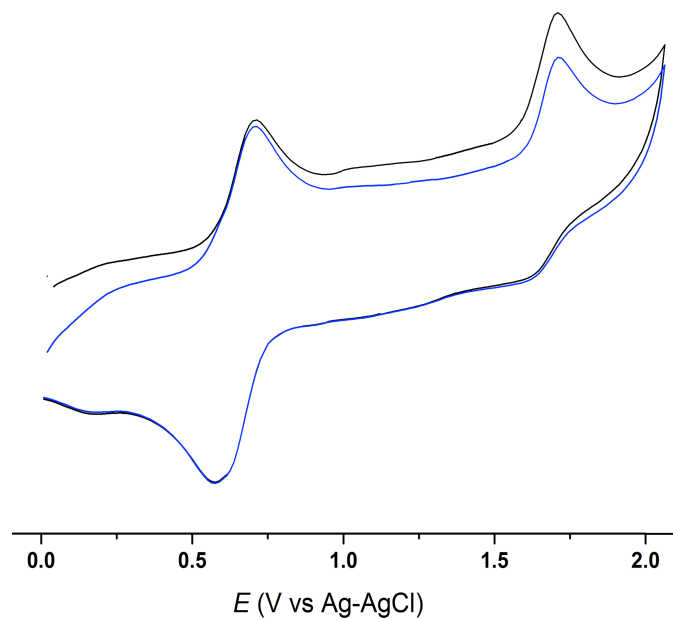


**Figure S6.** Cyclic voltammograms depicting the 1<sup>st</sup> (black) and 2<sup>nd</sup> (blue) scan for the oxidation process of complex salt **12** recorded at 100 mV s<sup>-1</sup> in MeCN 0.1 M in [N(C<sub>4</sub>H<sub>9</sub>-*n*)<sub>4</sub>]PF<sub>6</sub> at 293 K.

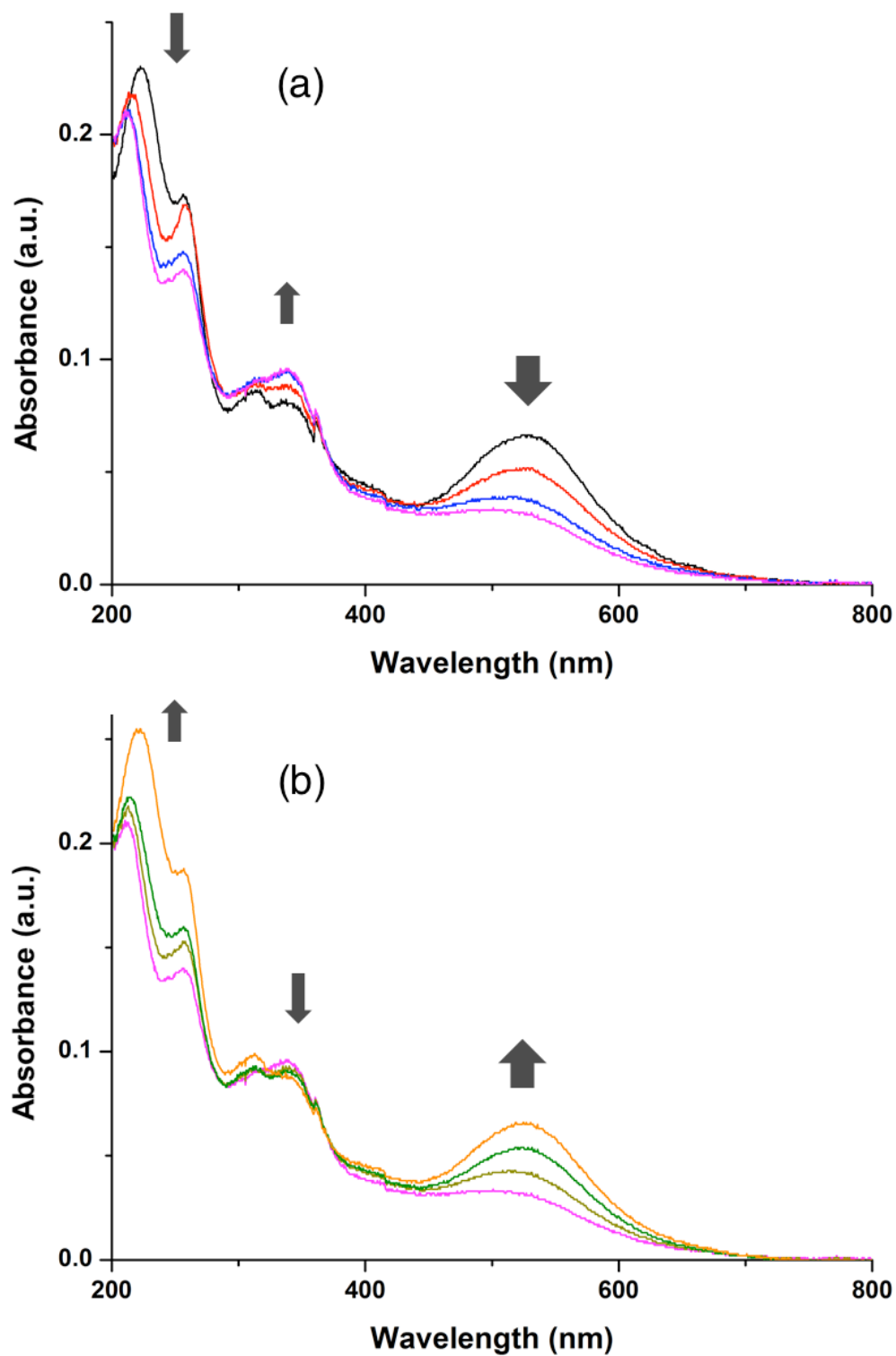


**Figure S7.** Spectroscopic changes upon oxidation at 1.0 V vs Ag–AgCl (a) followed by reduction at 0.0 V (b) of complex salt **11** (ca.  $10^{-4}$  M) in MeCN 0.1 M in  $[N(C_4H_9-n)_4]PF_6$  at 293 K in an OTTE cell.

#### 4. Additional Electronic Absorption and Emission Spectroscopic Data

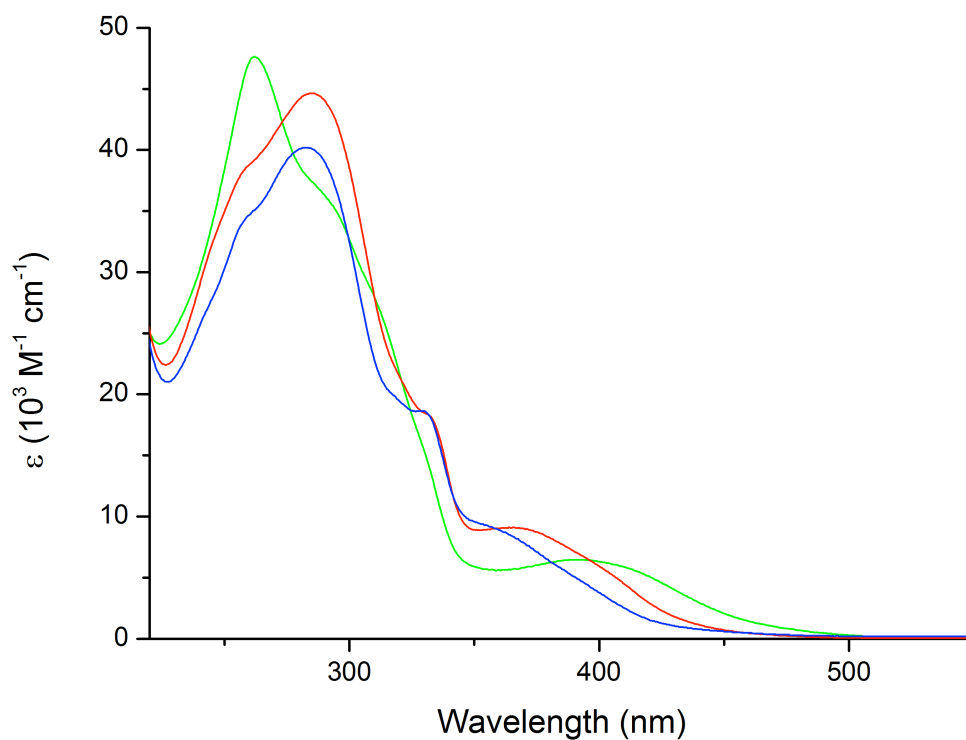


**Figure S8.** UV-vis absorption spectra of **5** (green), **6** (blue) and **7** (red) in MeCN at 293 K.

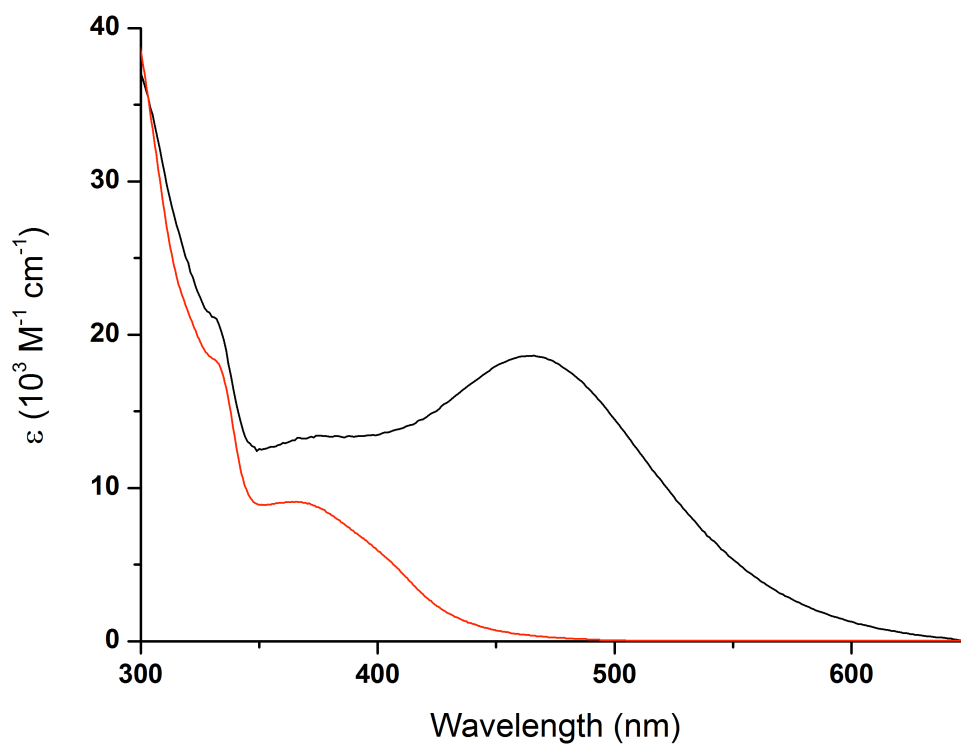


**Figure S9.** UV-vis absorption spectra of **7** (red) and **12** (black) in MeCN at 293 K.

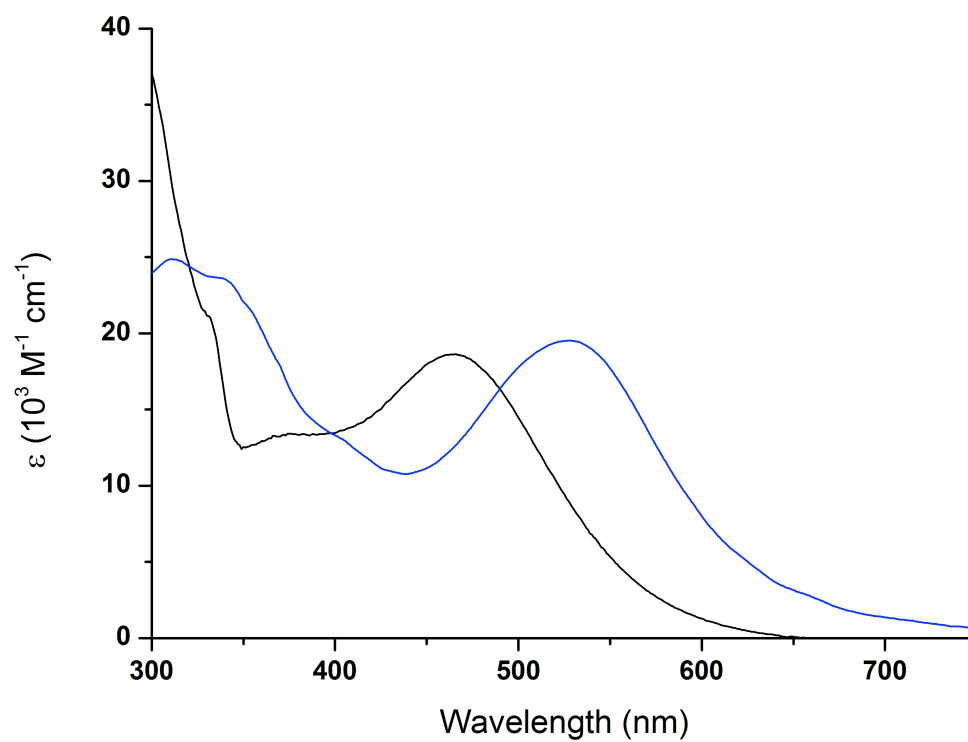


**Figure S10.** UV-vis absorption spectra of **11** (blue) and **12** (black) in MeCN at 293 K.

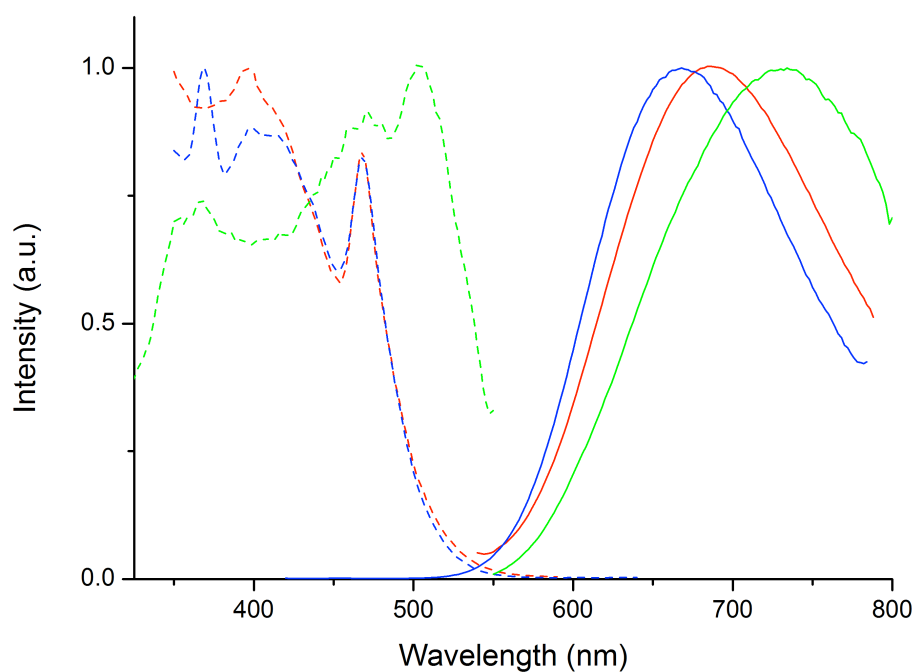


**Figure S11.** Emission (full lines) and excitation (dashed lines) spectra of the dc bpy-containing complex salts **2** (blue), **3** (green) and **4** (red) recorded in MeCN at 293 K.



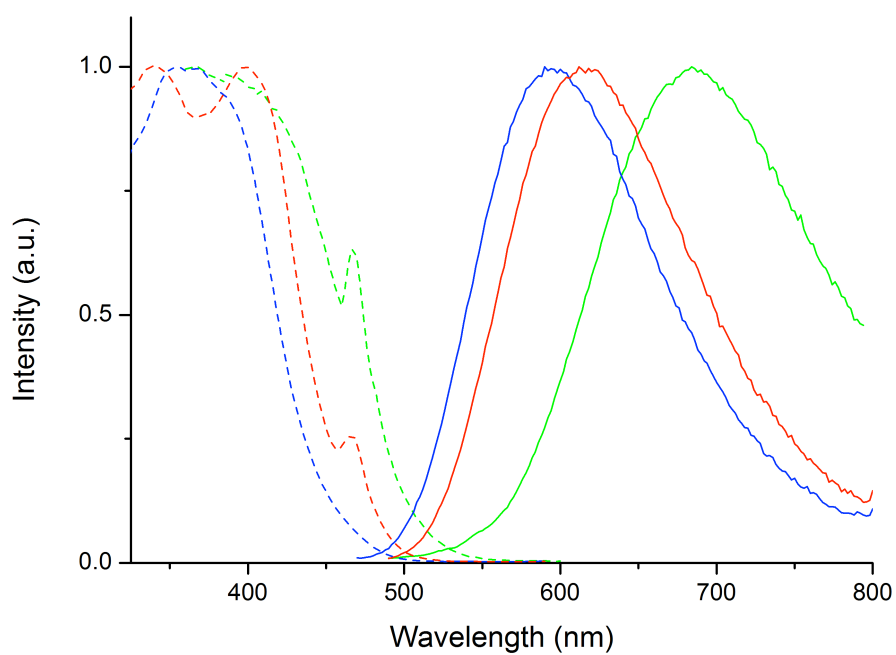


**Figure S12.** Emission (full lines) and excitation (dashed lines) spectra of the bcpbpy-containing complex salts **5** (green), **6** (blue) and **7** (red) recorded in MeCN at 293 K.

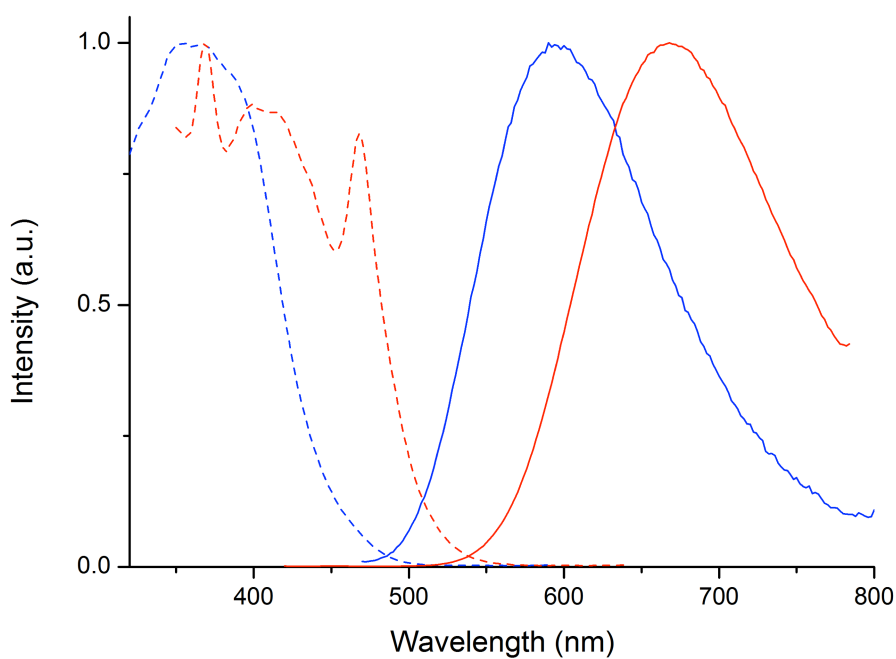


**Figure S13.** Emission (full lines) and excitation (dashed lines) spectra of the MeCN-containing complex salts **2** (red) and **6** (blue) recorded in MeCN at 293 K.

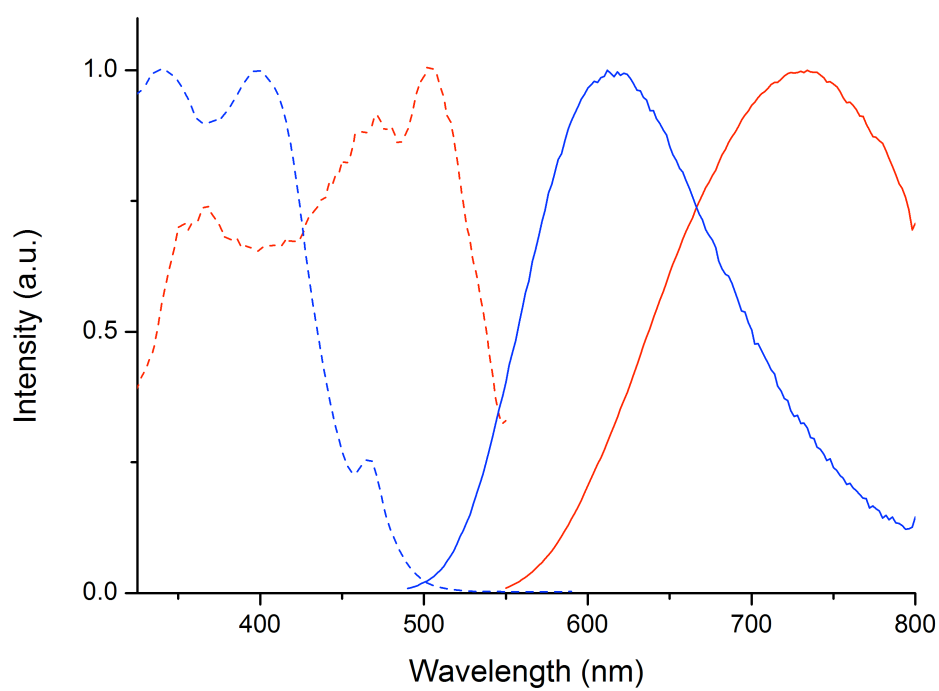


**Figure S14.** Emission (full lines) and excitation (dashed lines) spectra of the py-containing complex salts **3** (red) and **7** (blue) recorded in MeCN at 293 K.

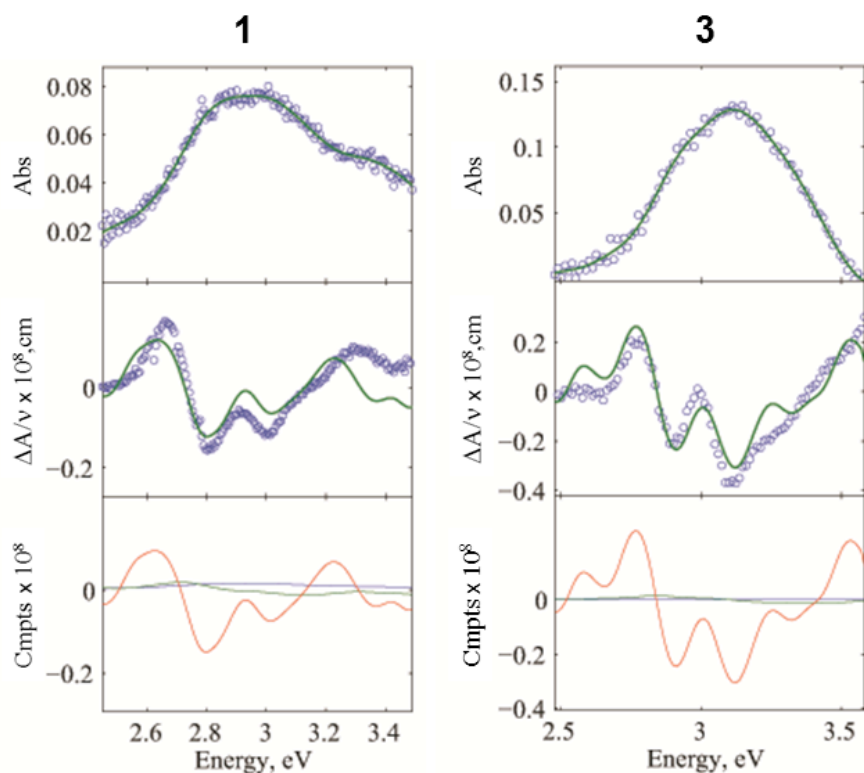


**Figure S15.** Spectra and calculated fits for the compounds **1** and **3** in PrCN at 77 K. Top panel: absorption spectrum; middle panel: electroabsorption spectrum, experimental (blue) and fits (green) according to the Liptay equation (Liptay, W. In *Excited States*, Vol. 1; Lim, E. C., Ed.; Academic Press, New York, 1974, pp. 129–229); bottom panel: contribution of 0th (blue), 1st (green) and 2nd (red) derivatives of the absorption spectrum to the calculated fits.